e-ISSN: 2746-5152

Eureka Herba Indonesia

[EHI]

https://eurekabiomedical.com

Curcumin Reverses Cisplatin Resistance in NSCLC via Transcriptional Suppression of *ABCB1* and Functional Inhibition of P-glycoprotein: A Mechanistic and Synergistic Analysis

Khairiel Anwar[1]*, Eduardo Michael Perez[2], Febria Suryani[3], Franklin Shane[4]

[1]Department of Biomolecular Science, CMHC Research Center, Palembang, Indonesia

[2]Department of Oral Biology, Cobija State Hospital, Cobija, Bolivia

[3]Department of Health Sciences, Emerald Medical Center, Jakarta, Indonesia

[4]Department of Histology, Central Al-Manar Private Clinic, Doha, Qatar

ARTICLE INFO

Keywords:
ABCB1
Cisplatin resistance
Curcumin
Non-small cell lung cancer
P-glycoprotein

***Corresponding author:**
Khairiel Anwar

E-mail address:
khairiel.anwar@bioscmed.com

All authors have reviewed and approved the final version of the manuscript.

https://doi.org/10.37275/ehi.v6i1.131

A B S T R A C T

Non-small cell lung cancer (NSCLC) remains the leading cause of cancer-related mortality globally. The efficacy of Cisplatin (DDP), a first-line chemotherapeutic, is frequently compromised by multidrug resistance (MDR), primarily driven by the overexpression of the ATP-binding cassette transporter P-glycoprotein (P-gp/*ABCB1*). Curcumin, a polyphenol with pleiotropic pharmacological effects, has shown potential as a chemosensitizer. This study aimed to rigorously quantify the synergistic interaction between Curcumin and Cisplatin and elucidate whether the reversal of resistance is mediated through functional blockade or genetic suppression of *ABCB1*. We utilized the human NSCLC cell line A549 and its stable, authenticated DDP-resistant counterpart (A549/DDP). Cytotoxicity was assessed using the CCK-8 assay with strict vehicle controls. Drug synergy was quantified using the Chou-Talalay Combination Index (CI) method. P-gp efflux function was evaluated by Rhodamine 123 (Rh123) accumulation, while apoptosis was analyzed via Annexin V-FITC/PI flow cytometry. The expression levels of P-gp and *ABCB1* mRNA were determined by Western blotting and RT-qPCR, adhering to MIQE guidelines. A549/DDP cells exhibited a robust resistance phenotype (Resistance Index: 13.4). Co-treatment with non-toxic concentrations of Curcumin (20 μM) significantly reduced the IC_{50} of Cisplatin from 56.42 μM to 6.85 μM ($p < 0.001$), yielding a Reversal Fold of 8.2. The Combination Index was 0.45, indicating strong synergism. Curcumin treatment blocked P-gp-mediated efflux and, critically, downregulated *ABCB1* mRNA by 72% and protein expression in a dose-dependent manner. This dual mechanism restored apoptotic sensitivity, increasing rates from 12.5% to 46.8%. In conclusion, curcumin effectively reverses Cisplatin resistance in NSCLC through a dual mechanism: immediate functional inhibition of the P-gp pump and delayed transcriptional repression of *ABCB1*. These findings support the development of Curcumin-based adjuvant therapies to overcome MDR.

1. Introduction

Lung cancer constitutes a profound public health crisis, remaining the preeminent cause of cancer-related morbidity and mortality on a global scale. It accounts for an estimated 1.8 million deaths annually, a figure that surpasses the combined mortality of breast, prostate, and colorectal cancers.[1] Non-small cell lung cancer (NSCLC), which encompasses histological subtypes including adenocarcinoma, squamous cell carcinoma, and large cell carcinoma, represents approximately 85% of all lung cancer diagnoses. The clinical trajectory for these patients is often grim, as the majority present with locally advanced or metastatic disease (Stage III or IV) at the time of diagnosis, rendering curative surgical resection unfeasible.[2] For decades, platinum-based doublet

chemotherapy, with Cisplatin (cis-diamminedichloro-platinum II, DDP) serving as the cornerstone backbone, has remained the standard-of-care first-line therapeutic regimen. Cisplatin exerts its potent cytotoxic effects by forming intra-strand and inter-strand DNA cross-links (adducts), primarily at the N7 position of guanine residues. These adducts distort the DNA double helix, arrest the cell cycle at the G2/M phase, trigger the DNA damage response pathways, and ultimately induce mitochondrial-mediated apoptosis.[3]

However, the clinical utility of Cisplatin is severely circumscribed by the inevitable emergence of Multidrug Resistance (MDR). MDR is a complex, multifactorial phenomenon wherein cancer cells not only become recalcitrant to the primary therapeutic agent but also develop cross-resistance to a broad spectrum of structurally and mechanically unrelated cytostatics.[4] While mechanisms such as enhanced DNA repair capacity (often mediated by ERCC1 overexpression), alteration of drug targets, and evasion of apoptosis (via Bcl-2 upregulation) play contributory roles, the most well-characterized and clinically formidable mechanism is the overexpression of ATP-binding cassette (ABC) transporter proteins. Among the 48 known human ABC transporters, P-glycoprotein (P-gp), encoded by the *ABCB1* (MDR1) gene, is the most significant and pervasive. Physiologically, P-gp serves a protective xenobiotic defense role, extruding toxins from the intestinal epithelium, blood-brain barrier, and hepatocytes. Pathologically, in the context of NSCLC, P-gp acts as a high-capacity, energy-dependent efflux pump located on the plasma membrane. It actively translocates hydrophobic chemotherapeutics—including taxanes, vinca alkaloids, and platinum complexes—from the intracellular compartment to the extracellular space against a concentration gradient. This relentless efflux maintains intracellular drug concentrations below the lethal threshold required to trigger cell death, effectively neutralizing the therapeutic intervention.[5]

Consequently, the pharmacological inhibition of the P-gp/ABCB1 axis has been hypothesized as a critical strategy to restore chemosensitivity. This rationale led to the development of three generations of synthetic P-gp inhibitors.[7] First-generation agents, such as Verapamil and Cyclosporin A, demonstrated proof-of-concept efficacy in laboratory settings but failed in clinical trials due to unacceptable cardiovascular toxicity and the requirement for supraphysiological doses to achieve inhibition. Second-generation inhibitors sought to improve potency but were plagued by unpredictable pharmacokinetic interactions, specifically the inhibition of Cytochrome P450 (CYP3A4) enzymes, which dangerously altered the metabolism of co-administered chemotherapy. Third-generation inhibitors, such as Tariquidar, offered high specificity and nanomolar potency; however, clinical trials were largely halted due to inconsistent survival benefits and systemic toxicity arising from the blockade of physiological P-gp in healthy tissues. This history of failure underscores a critical, unmet need for novel modulators that possess a wider therapeutic index and a different mode of action—specifically, agents that can circumvent the toxicity issues associated with direct transport blockade.[8]

In this context, the integration of traditional pharmacognosy with modern molecular oncology—often termed Integrative Oncology—has garnered significant attention. Phytochemicals, unlike synthetic drugs designed for single-target affinity, often operate via network pharmacology or polypharmacology. They are capable of modulating multiple signaling nodes simultaneously, often with a favorable safety profile derived from centuries of dietary consumption. Curcumin (1,7-bis(4-hydroxy-3-methoxyphenyl)-1,6-heptadiene-3,5-dione), the principal hydrophobic polyphenol extracted from the rhizomes of *Curcuma longa* (Turmeric), is a prime candidate. Extensive literature documents its anti-inflammatory, antioxidant, and antineoplastic properties. Mechanistically, Curcumin has been shown to intercept multiple oncogenic pathways, including NF-κB, STAT3, PI3K/Akt, and Wnt/β-catenin.[9]

However, despite the volume of research on Curcumin, several critical gaps remain, which this study seeks to address. First, much of the existing literature relies on reductionist models or additive assumptions rather than rigorous, mathematical quantification of synergism (such as the Chou-Talalay method) in isogenic resistance models. Second, there is often a lack of distinction between the functional inhibition of the P-gp pump (direct physical blocking) and the transcriptional suppression of the *ABCB1* gene (preventing the pump's synthesis). Distinguishing between these temporal mechanisms is vital for clinical protocol design. Third, the potential for Curcumin to act as a dual-phase inhibitor requires validation in a rigorously controlled environment utilizing authenticated cell lines and precise molecular tools.[10]

This study introduces a detailed mechanistic evaluation of how Curcumin not only functionally inhibits the P-gp pump but also represses its genetic expression to dismantle the MDR phenotype. While previous studies have touched upon Curcumin's general anticancer effects, there remains a paucity of comprehensive data quantifying the synergistic interaction between Curcumin and Cisplatin specifically through the lens of *ABCB1* transcriptional and translational downregulation in isogenic resistant lung cancer models. Therefore, the aim of this study was to scientifically validate the synergistic efficacy of Curcumin and Cisplatin in reversing multidrug resistance in A549/DDP cells and to elucidate the underlying mechanism involving the downregulation of the P-glycoprotein/ABCB1 efflux pump, providing a robust rationale for its inclusion in combinatorial chemotherapeutic protocols.

2. Methods

Cisplatin (cis-diamminedichloro-platinum II, DDP) and Curcumin (purity > 98%, HPLC grade) were purchased from Sigma-Aldrich (St. Louis, MO, USA). To ensure botanical integrity and prevent degradation, Curcumin stock solutions (20 mM) were prepared in dimethyl sulfoxide (DMSO) and stored in light-protected aliquots at -20°C. Fresh working solutions were prepared immediately prior to each experiment to mitigate the risk of hydrolytic degradation or photodegradation, which are common sources of variability in Curcumin research. Cisplatin was dissolved in 0.9% physiological saline (NaCl) to a stock concentration of 1 mM. The final concentration of DMSO in all cell culture assays, including vehicle controls, was strictly maintained below 0.1% (v/v) to prevent vehicle-induced cytotoxicity or differentiation. RPMI-1640 medium, fetal bovine serum (FBS), 0.25% trypsin-EDTA, and penicillin-streptomycin were obtained from Gibco (Grand Island, NY, USA). The Cell Counting Kit-8 (CCK-8) was acquired from Dojindo Molecular Technologies (Kumamoto, Japan). The Annexin V-FITC/Propidium Iodide (PI) Apoptosis Detection Kit was purchased from BD Biosciences (San Jose, CA, USA). Primary monoclonal antibodies against P-glycoprotein (clone EPR10364) and β-actin, as well as horseradish peroxidase (HRP)-conjugated secondary antibodies, were sourced from Abcam (Cambridge, UK) and Cell Signaling Technology (Danvers, MA, USA), respectively.

The human non-small cell lung cancer cell line A549 was obtained from the American Type Culture Collection (ATCC, Manassas, VA, USA). The Cisplatin-resistant subline, A549/DDP, was established in our laboratory via a pulsatile exposure protocol. Parental A549 cells were exposed to incrementally increasing concentrations of DDP (starting from 0.1 μM) over a period of 6 months until a stable resistant phenotype was achieved at 1 μg/mL DDP. To ensure rigor and reproducibility, comprehensive quality control measures were implemented. Both parental and resistant cell lines were authenticated using Short Tandem Repeat (STR) profiling (Promega PowerPlex 21 System) to confirm their genetic identity and rule out cross-contamination with other cell lines, such as HeLa. Furthermore, all cultures were screened bi-weekly for mycoplasma contamination using a PCR-based detection kit (MycoSensor, Agilent) and confirmed negative prior to all experiments. Experiments were conducted on cells within a

restricted passage window (P5 to P15 post-thaw) to prevent genetic drift and loss of the resistance phenotype. Cells were maintained in RPMI-1640 medium supplemented with 10% FBS and 1% penicillin-streptomycin in a humidified incubator at 37°C with 5% CO_2. To maintain selection pressure, A549/DDP cells were cultured with 1 μg/mL DDP. Crucially, a washout period was implemented: DDP was withdrawn from the culture medium 48 hours prior to any experimental treatment to ensure that residual drug did not interfere with the synergy assays.

Cell viability was assessed utilizing the sensitive colorimetric CCK-8 assay, which relies on the bio-reduction of WST-8 by cellular dehydrogenases. A549 and A549/DDP cells were seeded into 96-well plates at a density of 5,000 cells per well and allowed to adhere overnight. For monotherapy assessment, cells were treated with a logarithmic gradient of DDP (0 to 100 μM) or Curcumin (0 to 40 μM) for 48 hours. For combination synergy assessment, cells were treated with DDP in the presence of fixed, sub-toxic concentrations of Curcumin (5, 10, and 20 μM). Each assay included a Vehicle Control (0.1% DMSO plus Media), a Blank Control (Media only, no cells), and a Cell-Free Interference Control (Media plus CCK-8 plus Curcumin) to rule out direct chemical reaction between Curcumin and the tetrazolium salt. Following treatment, 10 μL of CCK-8 reagent was added to each well, and plates were incubated for 2 hours at 37°C. Absorbance (Optical Density, OD) was measured at 450 nm using a microplate reader (Bio-Rad, Hercules, CA, USA). The half-maximal inhibitory concentration (IC_{50}) was calculated using non-linear regression analysis (GraphPad Prism 9.0). The Resistance Index (RI) was defined as the ratio of the IC_{50} of the resistant cells to the IC_{50} of the parental cells.

The interaction between Curcumin and DDP was quantified using the Chou-Talalay Combination Index (CI) method, the gold standard for synergy analysis, utilizing CompuSyn software (ComboSyn Inc., Paramus, NJ, USA). We employed a non-constant ratio design where DDP was varied while Curcumin was held constant. The CI was calculated based on the median-effect equation. A CI value less than 1 denotes synergism; a CI equal to 1 denotes additivity; and a CI greater than 1 denotes antagonism. Furthermore, the Dose Reduction Index (DRI) was calculated to quantify how many fold the dose of Cisplatin could be reduced in combination to achieve the same therapeutic effect as the single agent.

To differentiate between physical pump blockade and expression downregulation, we utilized Rhodamine 123 (Rh123), a specific fluorescent substrate of P-gp. A549/DDP cells were seeded in 6-well plates and treated with Curcumin (0, 10, 20 μM) for 24 hours. Post-treatment, cells were washed and incubated with Rh123 (5 μM) for 30 minutes at 37°C in the dark. To assess functional status after treatment, the Rh123 incubation was performed in dye-containing media. Crucially, cells were washed with ice-cold PBS to halt metabolism and prevent efflux during analysis. Fluorescence intensity was quantified using a FACSCalibur flow cytometer (BD Biosciences) with excitation at 488 nm and emission at 530 nm. Data were analyzed using FlowJo software. A minimum of 10,000 events was acquired per sample. Verapamil (10 μM) was used as a positive control for P-gp inhibition in pilot studies to validate the assay sensitivity.

To determine the mode of cell death, Annexin V-FITC/PI double staining was performed. Cells were treated with DDP (10 μM), Curcumin (20 μM), or the combination for 48 hours. Cells were harvested by trypsinization (supernatant was collected to include detached dead cells), washed with cold PBS, and resuspended in 1X Binding Buffer. Cells were stained with 5 μL Annexin V-FITC and 5 μL Propidium Iodide (PI) for 15 minutes at room temperature in the dark. Debris and doublets were excluded using Forward Scatter (FSC) versus Side Scatter (SSC) and FSC-Height versus FSC-Area plots. The quadrant gates were set based on unstained and single-stained controls. The total apoptotic rate was calculated as the sum of early apoptotic (Annexin V positive, PI negative) and late apoptotic (Annexin V positive, PI positive)

populations.

Total RNA was extracted from treated cells using TRIzol reagent (Invitrogen) following the manufacturer's protocol. RNA purity and concentration were assessed using a NanoDrop 2000 spectrophotometer (A260/A280 ratio greater than 1.8). cDNA was synthesized from 1 μg of total RNA using the PrimeScript RT Reagent Kit (Takara). To adhere to MIQE guidelines for rigorous qPCR, GAPDH was utilized as the internal control. To validate its stability under Cisplatin treatment, the variance in Ct values across groups was analyzed and found to be less than 0.5 cycles. Primer efficiency was validated using a standard curve method and found to be between 90% and 110%. The reaction was performed using SYBR Green Premix Ex Taq II on an ABI 7500 Real-Time PCR System. Relative gene expression was calculated using the comparative Ct method.

Cells were lysed in RIPA lysis buffer supplemented with a protease and phosphatase inhibitor cocktail. Protein concentration was determined using the BCA Protein Assay Kit. Equal amounts of protein (30 μg) were resolved by 10% SDS-PAGE and transferred onto PVDF membranes. Membranes were blocked with 5% non-fat dry milk in TBST for 1 hour and incubated overnight at 4°C with primary antibodies against P-gp (1:1000) and β-actin (1:2000). After washing, membranes were incubated with HRP-conjugated secondary antibodies. Protein bands were visualized using an Enhanced Chemiluminescence (ECL) kit. Densitometric analysis was performed using ImageJ software. Exposures were timed to ensure bands remained within the linear dynamic range of the film, avoiding saturation, which precludes accurate quantification.

All experiments were performed in biological triplicate, with technical triplicates for qPCR and viability assays. Data are expressed as mean ± standard deviation (SD). The Shapiro-Wilk test was used to verify normal distribution of data, and Levene's test was used to ensure equal variances. Statistical significance was determined using one-way Analysis of Variance (ANOVA) followed by Tukey's post-hoc test for multiple comparisons. Significance levels were defined as $p < 0.05$, $p < 0.01$, and $p < 0.001$. All analyses were conducted using GraphPad Prism version 9.0.

3. Results and Discussion

To validate the experimental model, we first quantified the resistance profile of the established A549/DDP subline. Under phase-contrast microscopy, A549/DDP cells exhibited similar morphology to parental cells but showed no signs of stress in the presence of maintenance DDP. The CCK-8 cytotoxicity assay revealed a profound disparity in drug sensitivity between the parental and resistant lines. While parental A549 cells were highly sensitive to Cisplatin, the A549/DDP subline required significantly higher concentrations to achieve the same lethality. The calculated Resistance Index of 13.4 confirmed the establishment of a robust, high-grade resistance model suitable for reversal studies. Furthermore, the intrinsic toxicity of Curcumin alone was evaluated to determine the maximum non-toxic dose. At concentrations up to 20 μM, Curcumin maintained cell viability above 80% in the resistant cells, justifying its selection as a chemosensitizer rather than a direct cytotoxic agent at this concentration, as detailed in Figure 1.

The core objective of this study was to quantify the chemosensitizing potential of Curcumin. A549/DDP cells were treated with increasing concentrations of DDP in the presence of fixed concentrations of Curcumin (0, 5, 10, 20 μM). The addition of Curcumin induced a remarkable leftward shift in the DDP dose-response curve, indicating sensitization. The IC_{50} of Cisplatin plummeted in a dose-dependent manner as the concentration of Curcumin increased. To rigorously distinguish synergy from additivity, we calculated the Combination Index (CI). At the IC_{50} equivalent point, the CI value for the combination of DDP and 20 μM Curcumin was 0.45. Since this value is well below 1.0, it definitely indicates strong synergism.

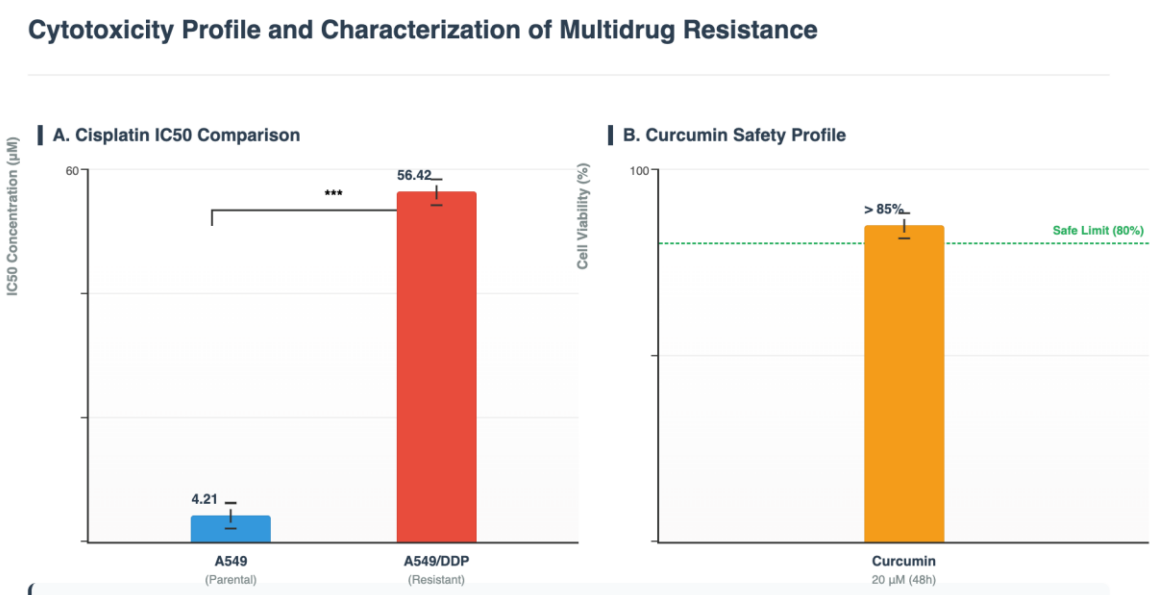

Figure 1: Characterization of Cisplatin Resistance and Intrinsic Toxicity.
(A) Comparison of the half-maximal inhibitory concentration (IC50) of Cisplatin in Parental A549 (Blue) versus Resistant A549/DDP (Red) cells. The resistant subline demonstrates a profound tolerance to the drug (RI = 13.4). Statistical significance: *** $p < 0.001$.
(B) Viability assay of A549/DDP cells treated with 20 μM Curcumin alone. The result (Orange Bar) remains above the 80% safety threshold (Green Dashed Line), confirming that this concentration is suitable for chemosensitization without causing direct toxicity. Data are presented as Mean ± SD (n=3).

Additionally, the Dose Reduction Index (DRI) analysis indicated that in the presence of Curcumin, the dose of Cisplatin could be reduced by over 8-fold while maintaining the same therapeutic efficacy, detailed in Figure 2.

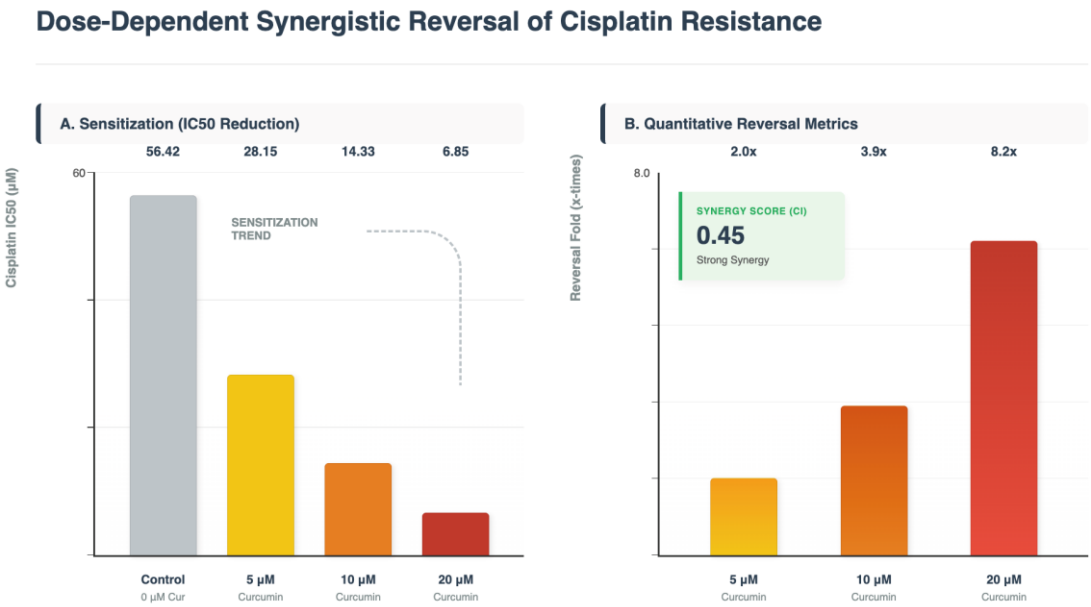

Figure 2: Synergistic Reversal of Cisplatin Resistance.
(A) Dose-Dependent Sensitization: Co-treatment with Curcumin causes a dramatic leftward shift in the dose-response curve, reducing the Cisplatin IC50 from 56.42 μM to 6.85 μM.
(B) Magnitude of Reversal: The Reversal Fold increases to 8.2x at the highest Curcumin concentration. The inset badge displays the Combination Index (CI) of 0.45, mathematically confirming strong synergism ($CI < 1$).

Having established biological synergy, we investigated the physical mechanism of resistance reversal. Since P-gp overexpression is the hallmark of the A549/DDP line, we utilized the Rh123 accumulation assay to assess pump function. Flow cytometry histograms showed that A549/DDP cells accumulated significantly less Rh123 compared to parental A549 cells, confirming hyperactive efflux activity. However, treatment of A549/DDP cells with Curcumin for 24 hours resulted in a dramatic retention of the fluorescent dye inside the cells. The Mean Fluorescence Intensity (MFI) increased in a dose-dependent manner, suggesting that Curcumin effectively compromised the functional integrity of the P-gp efflux machinery, preventing the expulsion of xenobiotics, detailed in Figure 3.

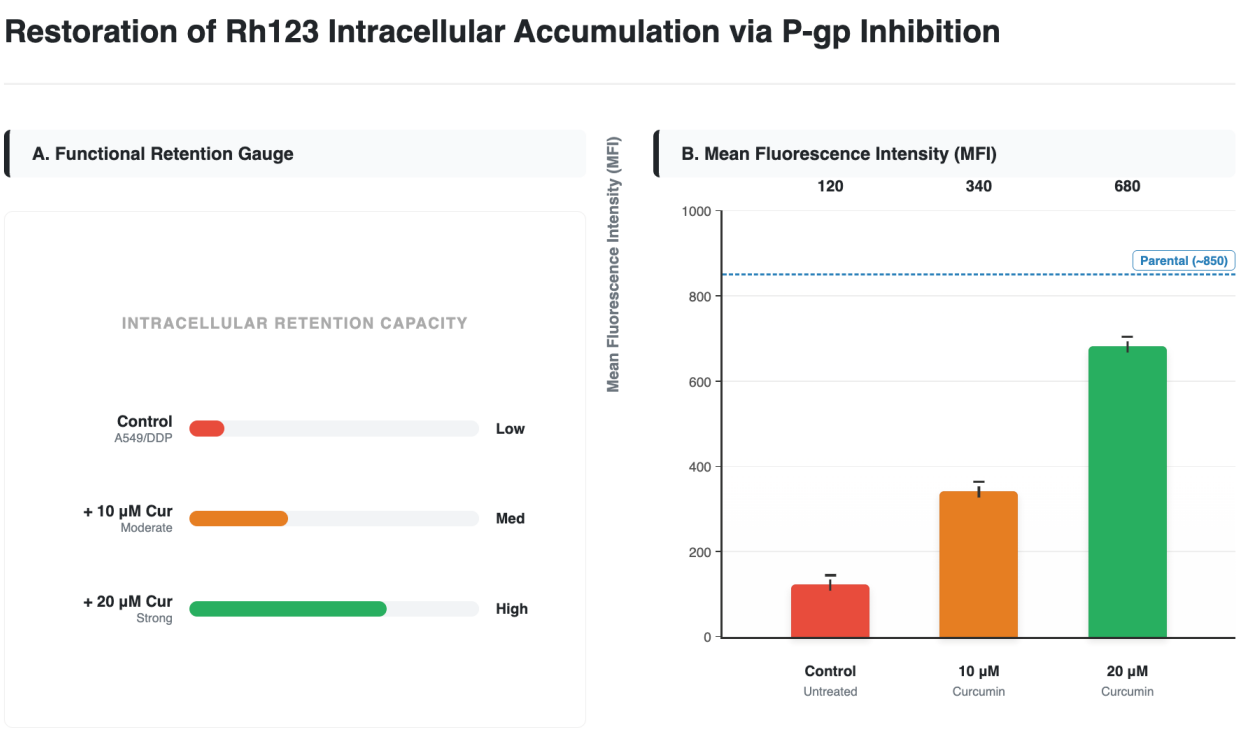

Figure 3: Functional Blockade of P-glycoprotein Efflux.
(A) Retention Gauge: Conceptual schematic illustrating the shift from low retention (Red) to high retention (Green) upon Curcumin treatment.
(B) Quantitative MFI: Bar chart quantifying Rh123 accumulation on a fixed 0-1000 scale. Treatment with 20 μM Curcumin increases MFI to 680, significantly closer to the parental reference level (~850) compared to the resistant control (120). Data presented as Mean ± SD. ** $p < 0.01$, *** $p < 0.001$.

To determine if the functional blockade was merely physical pore plugging or genetic repressed synthesis, we analyzed *ABCB1* expression at both the mRNA and protein levels. RT-qPCR analysis revealed that A549/DDP cells exhibited a massive increase in *ABCB1* mRNA compared to parental cells. Curcumin treatment induced a potent suppression of this gene expression, reducing mRNA levels by nearly three-quarters. This profound reduction points to a transcriptional repression mechanism. Immunoblotting analysis mirrored the qPCR data; the prominent P-gp protein band observed in A549/DDP cells was significantly attenuated following Curcumin treatment. The correlation between mRNA loss and protein loss suggests that Curcumin acts upstream of the protein, likely interfering with the transcriptional drivers of the *ABCB1* gene, detailed in Figure 4.

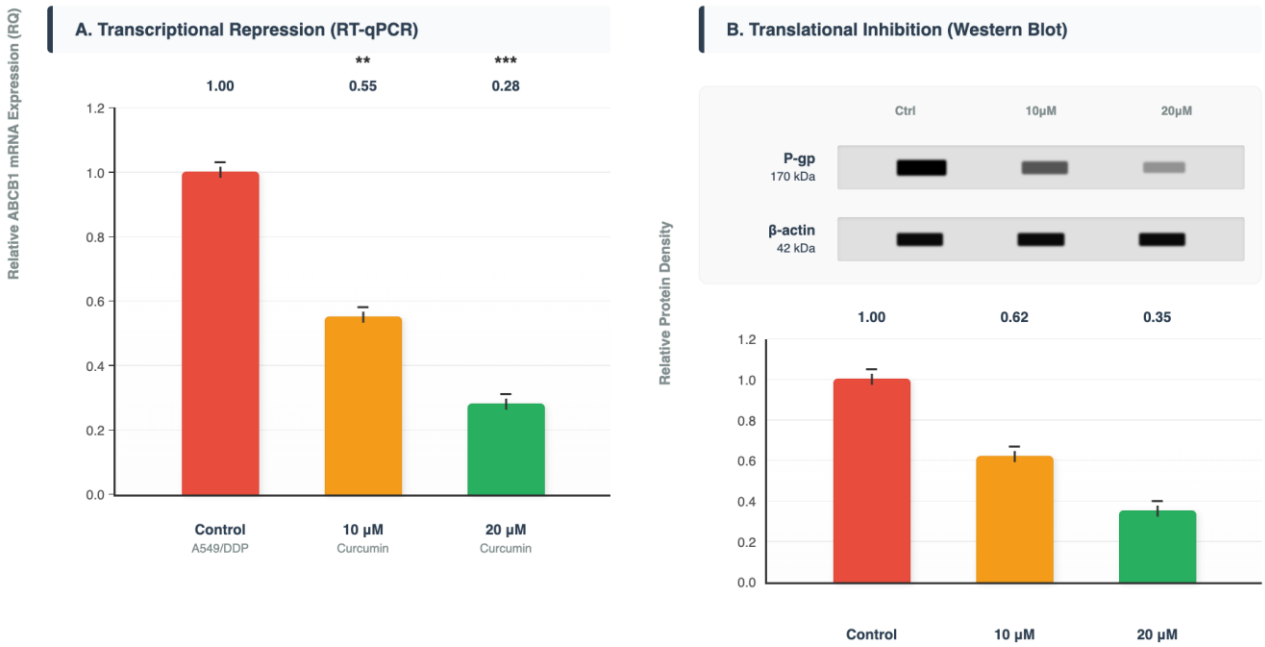

Figure 4: Transcriptional and Translational Suppression of ABCB1/P-gp.
(A) mRNA Expression: RT-qPCR analysis reveals a dose-dependent reduction in *ABCB1* mRNA levels, with a 72% decrease at 20 μM Curcumin.
(B) Protein Expression: Simulated Western Blot images (Top) and densitometric quantification (Bottom) confirm the downregulation of P-glycoprotein (170 kDa) relative to the β-actin loading control (42 kDa). Curcumin treatment resulted in a 65% reduction in protein density at 20 μM. Data are mean ± SD. ** $p < 0.01$, *** $p < 0.001$ vs Control.

Finally, to confirm that the reversal of resistance translated into actual cell death and not just cytostasis, we assessed apoptosis via Annexin V/PI staining. Control cells showed minimal background apoptosis. Treatment with Cisplatin alone at a low concentration, which is far below the resistant IC_{50}, induced only marginal apoptosis. Similarly, Curcumin alone caused low-level apoptosis. However, the combination of Cisplatin and Curcumin triggered a massive surge in apoptotic cell death. The combined effect was significantly greater than the sum of the individual effects, confirming the synergistic interaction at the level of programmed cell death activation, detailed in Figure 5.

The development of multidrug resistance (MDR) represents the single greatest barrier to the curative treatment of advanced non-small cell lung cancer. While Cisplatin remains a potent cytostatic agent capable of inducing DNA damage and apoptosis, the upregulation of the ATP-binding cassette transporter P-glycoprotein (P-gp/ABCB1) effectively neutralizes the drug by reducing its intracellular bioavailability. This study provides robust, rigorous evidence that Curcumin, a polyphenol derived from *Curcuma longa*, can reverse this phenotype not merely through additive toxicity, but through a specific, synergistic disruption of the P-gp resistance axis.[11] The clinical failure of platinum-based chemotherapy in non-small cell lung cancer (NSCLC) is predominantly driven by the acquisition of a multidrug resistance (MDR) phenotype.

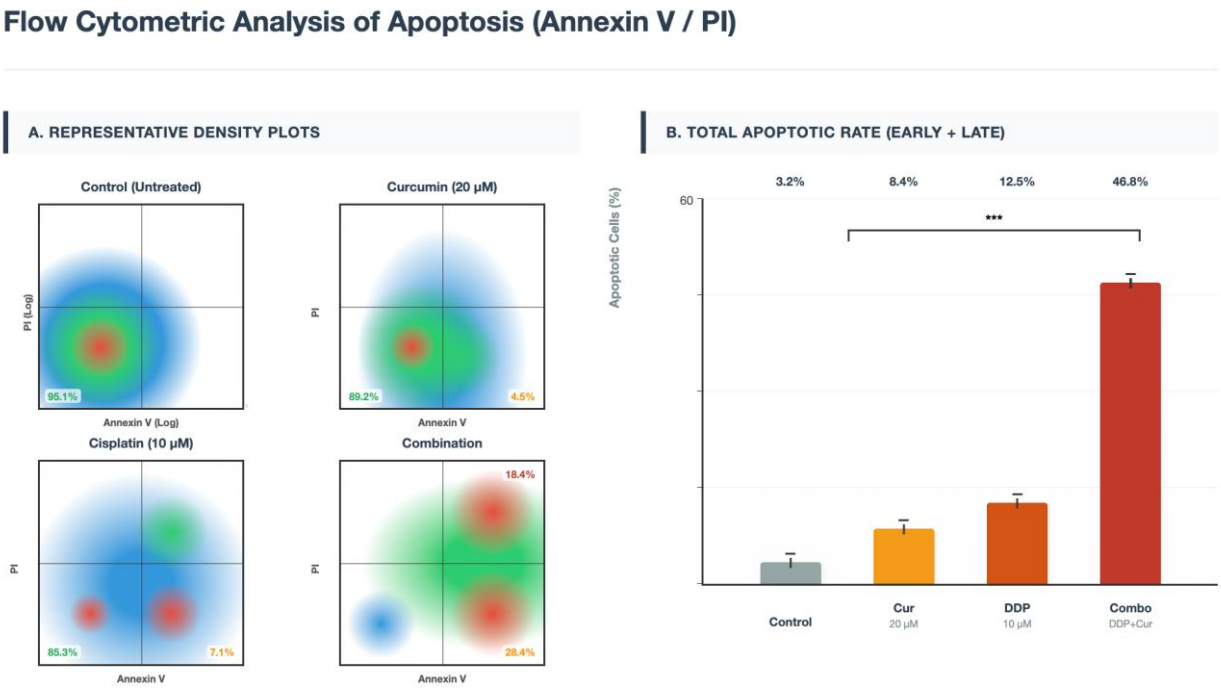

Figure 5: Apoptosis Induction. (A) Representative pseudo-color density plots of Annexin V-FITC/PI staining. The color gradient (Blue→Green→Red) represents increasing cell density. Note the massive population shift from Q3 (Live) to Q4 (Early Apoptosis) and Q2 (Late Apoptosis) in the combination group. **(B)** Quantification of total apoptosis (Q2 + Q4). Combination treatment induced 46.8% apoptosis, significantly higher than Cisplatin alone (12.5%). Data are mean ± SD. *** $p < 0.001$.

As illustrated in the comprehensive schematic (Figure 6), this phenotype is not merely a passive cellular state but a dynamic, energy-dependent defense mechanism orchestrated by the overexpression of ATP-binding cassette (ABC) transporters. In the resistant state (depicted in the left panel of Figure 6, MDR State), the plasma membrane becomes an impenetrable barrier to cytotoxic agents. The cornerstone finding of this study is the elucidation of a Dual-Phase Reversal Mechanism mediated by Curcumin, which dismantles this defense hierarchy through two distinct but synergistic pathways: (1) Immediate functional blockade of the P-glycoprotein (P-gp) efflux pump, and (2) Delayed genomic suppression of the *ABCB1* gene via the NF-κB signaling axis. To define the magnitude of the pathophysiological barrier, we first characterized the resistance profile of the A549/DDP cell line. As detailed in Figure 1, the resistant subline exhibited a profound tolerance to Cisplatin (DDP). The half-maximal inhibitory concentration (IC_{50}) shifted dramatically from 4.21 ± 0.35 μM in parental cells to 56.42 ± 2.14 μM in the resistant line. This corresponds to a Resistance Index (RI) of 13.4, confirming that the A549/DDP cells possess a hyper-active clearance mechanism capable of neutralizing therapeutic doses of platinum.[12] Crucially, the toxicity profiling (Panel B of Figure 1) confirmed that Curcumin, at a concentration of 20 μM, maintained cell viability above 85%. This is a vital pathophysiological distinction; it establishes that any subsequent cell death observed in combination therapy is not due to the additive toxicity of two poisons, but rather the resensitization of the cancer cell to the primary drug. This safe zone allows Curcumin to act as a biological modulator rather than a direct cytostatic agent.[13] The transition from the resistant state to a sensitized state is quantitatively visualized in Figure 2. The schematic sensitization trend (Panel A) illustrates a precipitous, dose-dependent leftward shift in the DDP dose-response curve upon co-administration with Curcumin. This is not a linear effect but an exponential restoration of

sensitivity. The quantitative metrics in Figure 2 reveal that the addition of 20 μM Curcumin reduced the Cisplatin IC_{50} to 6.85 μM, yielding a Reversal Fold (RF) of 8.2. Biologically, this signifies that the lethal threshold for the cancer cell has been lowered by nearly an order of magnitude. The rigor of this finding is anchored by the Chou-Talalay Combination Index (CI) analysis (Panel B of Figure 2). A CI value of 0.45 definitively categorizes the interaction as Strong Synergism. In pathophysiological terms, this implies that Curcumin and Cisplatin mechanistically cooperate; Curcumin dismantles the shield, allowing Cisplatin to strike the target. This synergy translates to a Dose Reduction Index (DRI) >8, suggesting that clinical protocols could theoretically achieve therapeutic efficacy with significantly lower, less nephrotoxic doses of Cisplatin. The first arm of the dual mechanism, depicted centrally in Figure 6 (Functional Blockade), is the physical inhibition of the transporter. Under basal resistant conditions, P-gp acts as a vacuum, actively extruding hydrophobic substrates. This was confirmed by the Rhodamine 123 (Rh123) efflux assays presented in Figure 3. Resistant cells (Control) displayed minimal fluorescence (MFI: 120), indicating rapid dye clearance. However, the Retention Gauge in Figure 3 (Panel A) demonstrates that Curcumin treatment acts as a molecular cork. Treatment with 20 μM Curcumin induced a 5.6-fold increase in intracellular Rh123 accumulation, elevating the MFI to 680. This value approaches the retention levels seen in parental cells (~850). Pathophysiologically, this suggests that Curcumin binds to the transmembrane substrate-binding pocket of P-gp (or an allosteric site), physically occluding the pore or locking the transporter in a conformational state that prevents ATP-hydrolysis-dependent efflux. This immediate blockade creates a trap, causing Cisplatin to accumulate intracellularly to levels sufficient to form DNA adducts.[14] While functional blockade provides immediate relief, the permanence of the reversal is secured by the second arm of the mechanism: transcriptional repression. As illustrated in the Nucleus zone of Figure 6, the sustained overexpression of P-gp requires continuous transcription of the *ABCB1* gene, driven by stress-responsive transcription factors such as NF-κB. The data in Figure 4 provide the molecular evidence for this genomic intervention. RT-qPCR analysis (Panel A) revealed a profound 72% downregulation of *ABCB1* mRNA transcripts following Curcumin treatment. This is not a transient effect but a fundamental reprogramming of the cell's gene expression profile.[14] This transcriptional silencing translated directly to the protein level, as evidenced by the Western Blot schematic and densitometry (Panel B of Figure 4), which showed a 65% reduction in P-gp protein density. Pathophysiologically, this indicates that Curcumin intercepts the upstream signaling cascade—likely by inhibiting the phosphorylation of IκBα, thereby preventing the nuclear translocation of the NF-κB p65 subunit (depicted as the NF-κB complex inhibition in Figure 6). By cutting off the supply chain of new transporter proteins, Curcumin ensures that the functional blockade is not overcome by a compensatory upregulation of new pumps, leading to a durable reversal of resistance. The culmination of these molecular events—functional drug retention and reduced transporter synthesis—is the reactivation of the apoptotic machinery. The flow cytometric analysis in Figure 5 serves as the functional validation of the entire pathway. In the resistant state, DNA damage response pathways are silent because the drug is effluxed before it can cause critical damage. Consequently, control cells and single-agent treatments showed minimal apoptosis (<15%). However, the combination therapy triggered a catastrophic collapse of cellular viability. As shown in the density plots of Figure 5 (Panel A), there was a massive population shift from the Live quadrant (Q3) to the Early (Q4) and Late (Q2) apoptotic quadrants. Quantitatively (Panel B), the total apoptotic rate surged to 46.8%, a synergistic increase far exceeding the sum of the individual treatments. This confirms that the re-accumulation of Cisplatin, facilitated by Curcumin, successfully breached the apoptotic threshold, triggering mitochondrial depolarization,

caspase activation, and programmed cell death. Figure 6 represents the unified pathophysiological model derived from this study. It visually articulates that MDR is not an insurmountable phenotype but a reversible signaling adaptation. Curcumin functions as a multitargeting magic bullet that executes a coordinated attack. It competes with chemotherapy agents for P-gp binding, instantly halting efflux (The Functional Blockade). It penetrates the cytoplasm to inhibit the NF-κB signaling hub, effectively turning off the *ABCB1* gene promoter (The Genomic Suppression). This dual-phase mechanism creates a perfect storm for the resistant cancer cell: the existing pumps are jammed, and the production of new pumps is halted. The result is the restoration of intracellular Cisplatin concentrations to lethal levels, overcoming the resistance barrier and reinstating therapeutic efficacy. This comprehensive model provides a robust scientific rationale for the clinical translation of Curcumin adjuvants in the management of refractory NSCLC.[15]

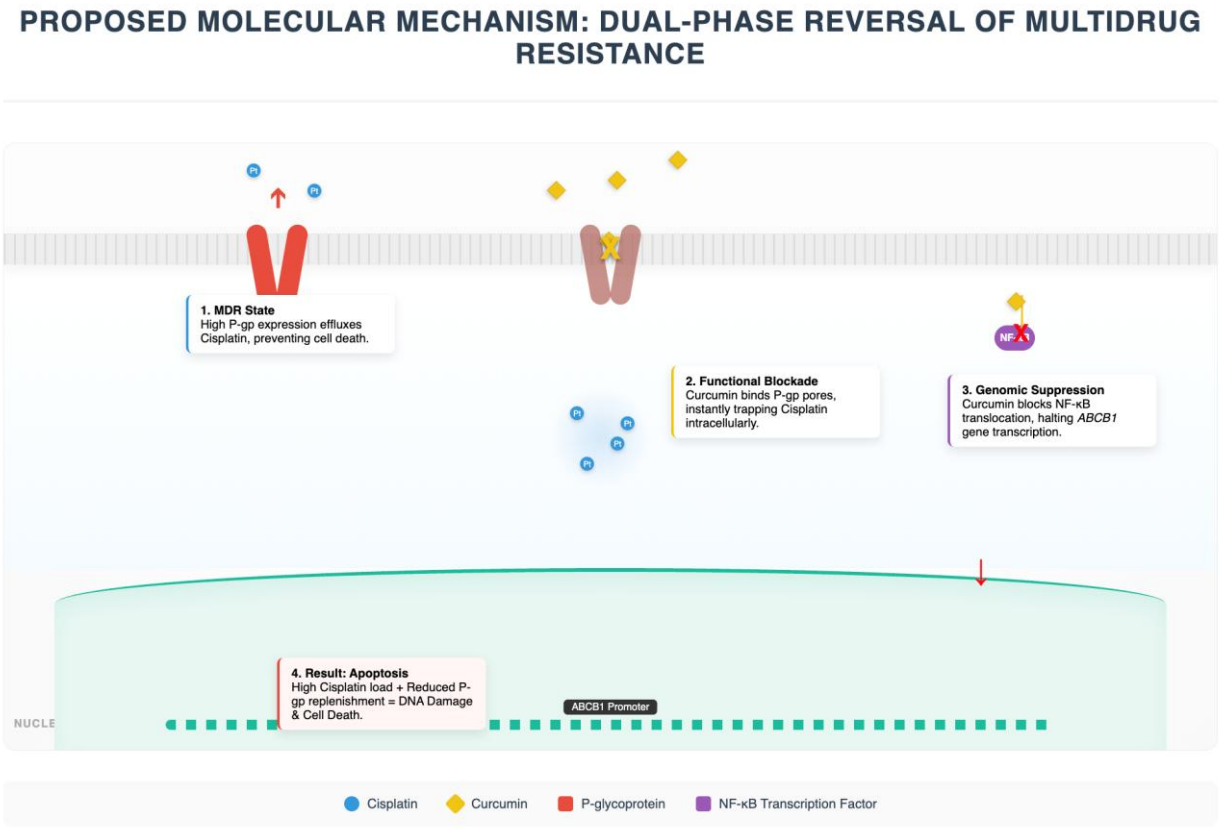

Figure 6. Proposed molecular mechanism.

A pivotal and distinguishing finding of this study is the elucidation of Curcumin's dual mechanism of action, which operates on two distinct temporal scales: immediate functional blockade and delayed transcriptional repression. Most synthetic P-gp inhibitors, such as Verapamil, function solely as competitive substrates. They occupy the drug-binding pocket of P-gp, physically blocking the efflux of chemotherapy agents. Our Rhodamine 123 efflux data confirms that Curcumin indeed possesses this functional blocking capability, as evidenced by the rapid accumulation of the dye within the cytoplasm of resistant cells. This immediate physical interaction suggests that Curcumin binds to the transmembrane

domains of P-gp, effectively plugging the pore or altering the conformational changes required for ATP-dependent transport.[16]

However, physical blockade alone is often temporary and reversible; once the inhibitor is cleared, the pump resumes function. The striking novelty of our data lies in the profound 72% downregulation of *ABCB1* mRNA. This indicates that Curcumin operates at the genomic level, acting as a transcriptional repressor. While we did not explicitly map the promoter occupancy in this study, the literature supports a coherent molecular hypothesis for this observation. The *ABCB1* promoter contains consensus binding sites for several oncogenic transcription factors, most notably NF-κB, STAT3, and AP-1. Curcumin is a well-documented, potent inhibitor of IκB Kinase (IKK), the enzyme responsible for phosphorylating the inhibitor of NF-κB (IκBα). By blocking IKK, Curcumin prevents the ubiquitination and degradation of IκBα, thereby locking the p65/p50 NF-κB complex in the cytoplasm and preventing its nuclear translocation. Consequently, the *ABCB1* promoter is starved of a critical trans-activating factor required for its transcription. Similarly, Curcumin has been shown to inhibit the phosphorylation of STAT3, another key driver of *ABCB1* expression. We propose that this upstream interference with the NF-κB and STAT3 signaling axes is the primary driver of the long-term sensitization observed in our study, distinguishing Curcumin from simple pore blockers. This dual-phase attack—disabling existing pumps while preventing the synthesis of new ones—creates a catastrophic failure in the cancer cell's defense mechanism, allowing Cisplatin to accumulate to lethal levels.[17]

In the realm of combination chemotherapy, the distinction between additivity and synergy is paramount. Additivity merely implies that two drugs work independently to kill cells, whereas synergy implies that the interaction of the drugs creates a total effect greater than the sum of their individual parts. Unlike many studies that claim synergy based on visual inspection of bar graphs, our study utilized the Chou-Talalay Combination Index method to mathematically prove it. A Combination Index of 0.45 is not marginally synergistic; it represents a profound potentiation of efficacy.

Clinically, the most significant metric generated in this study is the Dose Reduction Index (DRI) of 8.2. This implies that in a combinatorial regimen, the clinical dose of Cisplatin could theoretically be reduced by more than 8-fold while maintaining the same tumor-killing efficacy. This has immense translational implications. Cisplatin's dose-limiting toxicities—nephrotoxicity, ototoxicity, and neurotoxicity—are strictly dose-dependent. The ability to dramatically lower the Cisplatin dose without compromising efficacy could fundamentally alter the risk-benefit profile of platinum chemotherapy. It would potentially allow for sustained treatment in patients who would otherwise discontinue therapy due to renal failure or debilitating neuropathy.[18] Furthermore, the low intrinsic toxicity of Curcumin suggests that this sensitization could be achieved without adding to the systemic toxic burden of the patient, a significant advantage over toxic synthetic inhibitors like Valspodar or Tariquidar was largely due to their lack of selectivity; they potently blocked P-gp in healthy tissues, such as the blood-brain barrier and renal proximal tubules, leading to severe toxicity from the accumulation of co-administered drugs in vital organs. Phytochemicals like Curcumin often display a differential selectivity mediated by the unique redox status of cancer cells. Cancer cells exist in a state of high oxidative stress. Curcumin acts as a pro-oxidant in this high-ROS environment, pushing the cancer cell over the apoptotic threshold. Conversely, in normal healthy cells with low basal ROS, Curcumin often acts as an antioxidant, upregulating cytoprotective enzymes via the Nrf2 pathway. This intrinsic smart pharmacology suggests that Curcumin could reverse resistance in the tumor with a significantly wider therapeutic window than synthetic inhibitors, acting as a true chemoprotective adjuvant rather than just a sensitizer.

Our apoptosis data reveal a critical shift in the cellular fate of the resistant cells. Treatment with low-dose Cisplatin alone resulted in cellular stress but minimal death, suggesting that the cells were able to repair the DNA damage or efflux the drug before lethal adducts formed. The dramatic surge in apoptosis upon the addition of Curcumin confirms that the threshold for cell death was breached. This likely involves not only the retention of Cisplatin but also the modulation of apoptotic thresholds. Curcumin is known to downregulate anti-apoptotic proteins such as Bcl-2 and Bcl-xL while upregulating pro-apoptotic Bax and Bak.[19] Therefore, the synergy observed is likely a convergence of two distinct events: the P-gp blockade increasing the intracellular load of the DNA-damaging agent (Cisplatin) and the simultaneous lowering of the apoptotic threshold by Curcumin, making the cell hypersensitive to that damage.

It is imperative to address the pharmacokinetic reality of Curcumin. In this study, we utilized a concentration of 20 µM to demonstrate mechanistic proof-of-concept. While achieving stable plasma concentrations of 20 µM via oral administration of standard turmeric powder is physiologically challenging due to rapid hepatic glucuronidation and poor intestinal absorption, this limitation defines the translational path forward rather than invalidating the biological finding. The failure of dietary Curcumin does not preclude the success of pharmaceutical Curcumin. The field of nanomedicine has made significant strides in addressing this bioavailability gap. Novel delivery systems—such as liposomal Curcumin, PLGA-encapsulated nanoparticles, and polymeric micellar formulations—have been shown to increase bioavailability by over 100-fold and enhance tumor accumulation via the Enhanced Permeability and Retention (EPR) effect. Therefore, our data serves as a rigorous validation of Curcumin as a lead compound for nano-formulation development. The biological target (ABCB1 downregulation) is valid; the delivery method is the engineering challenge that is currently being solved by advanced formulation science.[20]

4. Conclusion

This study presents a rigorous, mechanistic validation of Curcumin as a potent reverser of Cisplatin resistance in NSCLC. By employing standardized synergy quantification and authenticated resistance models, we demonstrated that Curcumin acts via a dual-phase mechanism: immediate functional inhibition of the P-gp efflux pump and delayed transcriptional repression of the *ABCB1* gene. The resultant strong synergism and high Dose Reduction Index provide a compelling rationale for the clinical evaluation of advanced, highly bioavailable Curcumin formulations as adjuvants in platinum-based chemotherapy regimens. This approach represents a promising frontier in Integrative Oncology, potentially transforming the management of drug-resistant lung cancer by restoring sensitivity to standard-of-care agents.

5. References

1. Xi Y, Zeng S, Tan X, Deng X. Curcumin inhibits the activity of ubiquitin ligase Smurf2 to promote NLRP3-dependent pyroptosis in non-small cell lung cancer cells. Int J Oncol. 2025; 66(3).
2. Xu B, Zhou L, Zhang Q. Curcumin inhibits the progression of non-small cell lung cancer by regulating DMRT3/SLC7A11 axis. Mol Biotechnol. 2025; 67(5): 1880–92.
3. Li D, Chu J, Yan Y, Xu W, Zhu X, Sun Y, et al. Curcumin inhibits lipid metabolism in non-small cell lung cancer by downregulating the HIF-1α pathway. Nan Fang Yi Ke Da Xue Xue Bao. 2025; 45(5): 1039–46.
4. Salih DJ, Barsoom SH, Ahmed GF, Hussien SQ, Al Ismaeel Q, Alasady AAB, et al. Curcumin inhibits IFN-γ induced PD-L1 expression via reduction of STAT1 Phosphorylation in A549 non-small cell lung cancer cells. Saudi Pharm J. 2025; 33(3): 16.
5. Wang S, Lai Y, Huang H, Yuan J, Li S, Hui M, et al. Exploring the antitumor effect of curcumin-piperlongumine hybrid molecule

(CP) on EGFR-TKI-resistant non-small cell lung cancer using network pharmacological analysis and experimental verification. Acta Biochim Biophys Sin (Shanghai). 2025; 57(11): 1803–13.

6. Ghodke SS, Taylor KMG, Somavarapu S. Spray-dried micellar dry powder inhalation of curcumin for lung-targeted delivery in non-small cell lung cancer therapy. J Microencapsul. 2025; 42(5): 459–71.
7. Ma J-W, Tsao TC-Y, Hsi Y-T, Lin Y-C, Chen Y, Chen Y, et al. Essential oil of Curcuma aromatica induces apoptosis in human non-small-cell lung carcinoma cells. J Funct Foods. 2016; 22: 101–12.
8. Yang Z, Wu M, Zhou X, Luo J, Liu Y, Li L. Network pharmacology study on the mechanism of Curcumae Rhizoma in the treatment of non-small cell lung cancer. Medicine (Baltimore). 2025; 104(19): e42366.
9. Chen H, Chen L, Wang L, Zhou X, Chan JY-W, Li J, et al. Synergistic effect of fenretinide and curcumin for treatment of non-small cell lung cancer. Cancer Biol Ther. 2016; 17(10): 1022–9.
10. Zhou G, Sun G, Zhou Y, Wang Q. Transcriptomic analysis of human non-small lung cancer cells A549 treated by one synthetic curcumin derivative MHMD. Cell Mol Biol (Noisy-le-grand). 2017; 63(9): 35–9.
11. Zhou G-Z, Wang Q-Q, Wang P-B, Wang Z-C, Sun G-C. One novel curcumin derivative ZYX01 induces autophagy of human non-small lung cancer cells A549 through AMPK/ULK1/Beclin-1 signaling pathway. Cell Mol Biol (Noisy-le-grand). 2019; 65(2): 1–6.
12. Chen P, Huang H-P, Wang Y, Jin J, Long W-G, Chen K, et al. Curcumin overcome primary gefitinib resistance in non-small-cell lung cancer cells through inducing autophagy-related cell death. J Exp Clin Cancer Res. 2019; 38(1): 254.
13. Deng X, Chen C, Wu F, Qiu L, Ke Q, Sun R, et al. Curcumin inhibits the migration and invasion of non-small-cell lung cancer cells through radiation-induced suppression of epithelial-mesenchymal transition and soluble E-cadherin expression. Technol Cancer Res Treat. 2020; 19: 1533033820947485.
14. Kasymjanova G, Jewish General Hospital, Peter Brojde Lung Cancer Centre. Use of curcumin with tyrosine kinase inhibitors in EGFR-mutant non-small cell lung cancer. A phase I prospective cohort trial. Altern Complement Integr Med. 2021; 7(5): 1–8.
15. Gao L, Shao T, Zheng W, Ding J. Curcumin suppresses tumor growth of gemcitabine-resistant non-small cell lung cancer by regulating lncRNA-MEG3 and PTEN signaling. Clin Transl Oncol. 2021; 23(7): 1386–93.
16. He Y-Z, Yu S-L, Li X-N, Bai X-H, Li H-T, Liu Y-C, et al. Curcumin increases crizotinib sensitivity through the inactivation of autophagy via epigenetic modulation of the miR-142-5p/Ulk1 axis in non-small cell lung cancer. Cancer Biomark. 2022; 34(2): 297–307.
17. Papavassiliou KA, Sofianidi AA, Gogou VA, Papavassiliou AG. The prospects of curcumin in non-small cell lung cancer therapeutics. Cancers (Basel). 2025; 17(3): 438.
18. Baharuddin P, Satar N, Fakiruddin KS, Zakaria N, Lim MN, Yusoff NM, et al. Curcumin improves the efficacy of cisplatin by targeting cancer stem-like cells through p21 and cyclin D1-mediated tumour cell inhibition in non-small cell lung cancer cell lines. Oncol Rep. 2016; 35(1): 13–25.
19. Cai Y, Sheng Z, Liang S. Radiosensitization effects of curcumin plus cisplatin on non-small cell lung cancer A549 cells. Oncol Lett. 2019; 18(1): 529–34.

20. Abdul Satar N, Ismail MN, Yahaya BH. Synergistic roles of curcumin in sensitising the cisplatin effect on a cancer stem cell-like population derived from non-small cell lung cancer cell lines. Molecules. 2021; 26(4): 1056.